PNAS RESEARCH ARTICLE | IMMUNOLOGY AND INFLAMMATION

Aflatoxin B1 and Epstein–Barr virus-induced CCL22 expression stimulates B cell infection

Mohamed Ali Maroui[a,1], Grace Akinyi Odongo[b,1], Lucia Mundo[c,d], Francesca Manara[b], Fabrice Mure[a], Floriane Fusil[a], Antonin Jay[b], Tarik Gheit[b], Thanos M. Michailidis[e], Domenico Ferrara[d], Lorenzo Leoncini[d], Paul Murray[c], Evelyne Manet[a], Théophile Ohlmann[a], Marthe De Boevre[e], Sarah De Saeger[e,f], François-Loïc Cosset[a], Stefano Lazzi[d], Rosita Accardi[b,2], Zdenko Herceg[b,3,4], Henri Gruffat[a,3,4], and Rita Khoueiry[b,3,4]

Edited by Ethel Cesarman, Weill Medical College of Cornell University, New York, NY; received August 21, 2023; accepted February 20, 2024 by Editorial Board Member Yuan Chang

Epstein–Barr Virus (EBV) infects more than 90% of the adult population worldwide. EBV infection is associated with Burkitt lymphoma (BL) though alone is not sufficient to induce carcinogenesis implying the involvement of co-factors. BL is endemic in African regions faced with mycotoxins exposure. Exposure to mycotoxins and oncogenic viruses has been shown to increase cancer risks partly through the deregulation of the immune response. A recent transcriptome profiling of B cells exposed to aflatoxin B1 (AFB1) revealed an upregulation of the Chemokine ligand 22 (CCL22) expression although the underlying mechanisms were not investigated. Here, we tested whether mycotoxins and EBV exposure may together contribute to endemic BL (eBL) carcinogenesis via immunomodulatory mechanisms involving CCL22. Our results revealed that B cells exposure to AFB1 and EBV synergistically stimulated CCL22 secretion via the activation of Nuclear Factor-kappa B pathway. By expressing EBV latent genes in B cells, we revealed that elevated levels of CCL22 result not only from the expression of the latent membrane protein LMP1 as previously reported but also from the expression of other viral latent genes. Importantly, CCL22 overexpression resulting from AFB1-exposure in vitro increased EBV infection through the activation of phosphoinositide-3-kinase pathway. Moreover, inhibiting CCL22 in vitro and in humanized mice in vivo limited EBV infection and decreased viral genes expression, supporting the notion that CCL22 overexpression plays an important role in B cell infection. These findings unravel new mechanisms that may underpin eBL development and identify novel pathways that can be targeted in drug development.

CCL22 | mycotoxins | Epstein–Barr virus | endemic Burkitt lymphoma | carcinogenesis

Significance

This study provides an insight into the synergistic impact of exposures to environmental agents commonly present in the lymphoma belt regions in Africa such as aflatoxin B1 (AFB1) and oncogenic virus infection, e.g., Epstein–Barr virus (EBV). It reveals mechanisms through which these exposures might contribute to eBL. A focus here is on eBL development in which EBV infection plays a pivotal role together with co-factors such as AFB1 exposure. Our findings have unraveled a role for the AFB1-induced upregulation of the CCL22 in enhancing EBV infection of B cells and therefore a putative role in eBL development. This might corroborate what happens in African sub-Saharan regions where children are first exposed to mycotoxins including AFB1 through food contamination that could deregulate their immune response including CCL22 levels and increase their susceptibility to EBV infection. This would explain in part the high prevalence of eBL in those regions. Moreover, our in vitro and in vivo analyses provide promising evidence for the possible use of CCL22 as a drug target to inhibit eBL development.

Epstein–Barr virus (EBV), a member of the gamma herpesvirus family was the first human tumor virus identified in 1964 in a Burkitt lymphoma (BL). Subsequently, it was also found to be associated with other types of lymphomas (hodgkin lymphoma (HL), T and natural killer (NK)/T cell lymphoma) and carcinomas (nasopharyngeal carcinoma and a subset of gastric cancer) (1–4). EBV infects over 90% of the adult human population worldwide (5). While primary infection typically occurs during infancy in developing countries, it may be delayed until young adulthood in more industrialized nations. After infection, the virus persists in the memory B cells of the peripheral blood (6) undergoing two distinct phases in its life cycle: latency and lytic replication (6). During the latent phase, the viral genome is usually maintained as a circular episome in the cell nucleus and latent viral genes are expressed such as the latent membrane protein genes (i.e., *LMP1*) (7). Under certain conditions including those triggering immunodeficiency or cell differentiation, the viral lytic cycle is activated, and all viral genes are expressed resulting in the production of unique infectious virus particles (8–10). The virus then spreads to other host cells leading to increased EBV infection (11, 12). The viral genes expressed have varied potencies and may affect multiple signaling cascades accompanied by genetic and/or epigenetic changes leading to B cell transformation which may contribute to B cell lymphomagenesis (11). EBV lytic proteins (e.g., BPLF1) have been associated with B cell transformation through processes that affect viral DNA replication, viral infectivity, DNA repair, and immune evasion (13).

EBV infection is usually asymptomatic, however, under specific conditions [e.g., genetic mutations, immunosuppression, or co-exposure with one or more environmental factors such as co-infections with other biological agents or food contaminations (14)], the infection can result in the development of EBV-associated cancers (9, 15, 16). This is notably the case in endemic Burkitt lymphoma (eBL) which is predominantly localized in the so-called lymphoma belt of sub-Saharan Africa (17), a region with high malaria risk overlay.

[1]M.A.M. and G.A.O. contributed equally to this work.

[2]Deceased on 13 May 2020.

[3]Z.H., H.G., and R.K. contributed equally to this work.

[4]To whom correspondence may be addressed. Email: khoueiryr@iarc.who.int, henri.gruffat@ens-lyon.fr, or hercegz@iarc.who.int.

This article contains supporting information online at https://www.pnas.org/lookup/suppl/doi:10.1073/pnas.2314426121/-/DCSupplemental.

Published April 4, 2024.

Downloaded from https://www.pnas.org by UNIVERSITEITSBIBLIOTHEEK GENT on June 6, 2024 from IP address 157.193.59.67.

However, other risk factors involved in the etiology of eBL are suspected such as mycotoxins (toxins produced by fungi) particularly aflatoxins (18). Indeed, people living in the lymphoma belt are also chronically exposed to mycotoxins including aflatoxins (19). This exposure starts during gestation through the maternal diet and early in childhood life when solid foods are introduced, and is further continued in adulthood (20, 21). Aflatoxin B1 (AFB1) and AFB2 are both mycotoxins produced by *Aspergillus* species of fungi (22), though AFB2 is known to be less potent than AFB1 (23). In aflatoxins biosynthesis pathway, sterigmatocystin (STC) is a precursor of AFB1 while aflatoxicol (AFL) is one of the downstream metabolites of AFB1 (24–26). AFB1 has been clearly shown to synergize with hepatitis B virus in the development of hepatocellular carcinoma (27). However, little is known about the impact of AFB1 on B cell transformation and its possible synergistic role with EBV leading to eBL development. We have recently revealed several genes to have their expression altered in cells treated with AFB1 such as the immune-regulatory cytokine C–C motif chemokine ligand 22 (CCL22) (28) and TGFBI (29). Our study also showed that AFB1 and EBV play a synergistic role in downregulating TGFBI gene expression in B cells, revealing potential mechanisms of B cell transformation shared by those two risk factors of eBL (29). Yet, it is unclear whether the synergy of both exposures affects the expression of other genes. Moreover, our recent study conducted using in vitro models and a humanized mice model showed that exposure to AFB1 stimulates EBV infection and EBV-mediated B cell transformation (28). However, the mechanism by which AFB1 enhances B cell infection by EBV has not been determined. The induction of *CCL22* by AFB1 is particularly intriguing. CCL22 is a secreted protein that exerts chemotactic activity for monocytes, dendritic cells, NK cells, and for activated T lymphocytes. CCL22 seems also to be required in B cells to complete affinity maturation in germinal centers (30). Studies have reported that *CCL22* expression is induced in cells infected by different viruses such as human cytomegalovirus (CMV) as a viral mechanism to escape immune surveillance (31). Moreover, accumulating evidence indicates that CCL22 plays a tumor-promoting role in several human cancers (32–34). For example, high levels of circulating CCL22 are found in lymphomas (35) and in gastric cancer (36). In ovarian cancer, CCL22 was found to recruit regulatory T (T-reg) cells into the tumor mass and inhibit T cell immunity (35). At the molecular level, binding of CCL22 to its receptor, CCR4, leads to activation of the PI3K pathway that is often altered in cancer. However, the mechanisms of *CCL22* upregulation by AFB1 are not clear. Remarkably, EBV also has been shown to induce *CCL22* expression (37, 38) but whether AFB1-induced *CCL22* plays a role in EBV infection and B cell transformation contributing to eBL is not known.

Here, we revealed that CCL22 is overexpressed in B cells exposed to EBV and AFB1 and in EBV-associated BL tumors. Further, we used in vitro cultured B cells and a humanized mice model to conduct mechanistic studies aimed at revealing the mechanisms by which AFB1 and EBV stimulate CCL22 expression and secretion. We also studied the impact of this upregulation on EBV B cell infection. Both AFB1 and EBV were found capable of stimulating CCL22 in part via the activation of NF-kB pathway. Moreover, we have shown that CCL22 upregulation resulting from AFB1-exposed cells in vitro increases EBV infection. Therefore, we have questioned whether inhibiting CCL22 function would impact EBV infections and shown that neutralizing CCL22 function in vitro and in vivo indeed limits EBV infection. These results provide important mechanistic insights into the synergistic impact of EBV and mycotoxins on B cells that may underpin B cell transformation and contribute to eBL. This corroborates the possible role of AFB1 as an EBV co-factor in eBL development. Our study also reveals pathways that can be targeted in drug development for cancer.

Results

Mycotoxins Exposure and EBV Infection Impact *CCL22* Expression. We have previously observed that B cells exposed to aflatoxin B1 (AFB1) have altered gene expression profile compared to unexposed cells or to cells exposed to the less genotoxic aflatoxin B2 (AFB2) (28). Among the genes deregulated by exposure to AFB1, we identified *CCL22* being overexpressed in exposed cells. To validate these data, we first treated primary B cells or an EBV-negative Burkitt lymphoma B cell line (Louckes cells) with AFB1 or AFB2 and using DMSO as control. At 48 h after treatment, the cells were collected, as well as their culture supernatant. We investigated the expression levels of intracellular *CCL22* mRNA and protein as well as of the secreted cytokine level. In line with our previously published data (28), RT-qPCR and immunoblotting analyses confirmed that cells exposed to AFB1 and not AFB2 had higher intracellular expression levels of *CCL22* (Fig. 1 *A* and *B*) than non-exposed cells. We have also determined the levels of secreted cytokines by ELISA and western blot (WB) after Immunoprecipitation on the supernatant (Fig. 1*B*). All approaches revealed higher *CCL22* expression and CCL22 secretion from the AFB1-treated B cells compared with the DMSO-treated (control) cells. Further, we determined whether exposure of B cells to an AFB1 metabolite or precursor would also result in an increase in *CCL22* expression. To this end, we exposed primary B cells or Louckes cells to the AFB1 precursor sterigmatocystin (STC) or one of AFB1 metabolites aflatoxicol (AFL) or the combination of both compounds (AFL+ STC) (24–26, 39), and measured *CCL22* expression. Following 48 h of exposure, while a slight increase in *CCL22* expression was observed, this increase was generally not significant and lower than the increase observed following AFB1 exposure (Fig. 1 *C* and *D*). Because several viruses have been described to induce secretion of CCL22 as part of a viral strategy to counteract the host's immune surveillance, we next evaluated the impact of EBV infection on *CCL22* expression and observed a significant increase following infection (Fig. 1 *C* and *D*).

As epidemiological evidence shows an overlap between the so-called "lymphoma belt" region and areas heavily co-exposed to both AFB1 and EBV, we aimed to test whether both exposures could have a synergistic impact on *CCL22* expression. To mimic real life exposure to AFB1 and EBV in those areas where infants are first exposed to mycotoxins then infected with EBV, we first exposed primary B cells and Louckes cells to AFB1 (or its precursor STC and/or metabolite AFL) for 24 h then infected them or not with EBV for 24 h. We observed a significant enhancement of *CCL22* expression when cells were exposed to both AFB1 and EBV. This suggests a synergy between AFB1 exposure and EBV infection in regulating *CCL22* expression (Fig. 1 *C* and *D*).

Because secreted CCL22 may bind to the CCR4 receptor, potentially attracting Th2 cells and regulatory T cells (38), thus inhibiting Th1 cytotoxic response, we assessed a possible change in the CCR4 receptor gene expression levels following exposure of Louckes or primary B cells to AFB1 and infection with EBV. Our results showed an increase in *CCR4* expression that is significant following EBV infection (Fig. 1*E*), suggesting an augmentation of

Downloaded from https://www.pnas.org by UNIVERSITEITSBIBLIOTHEEK GENT on June 6, 2024 from IP address 157.193.59.67.

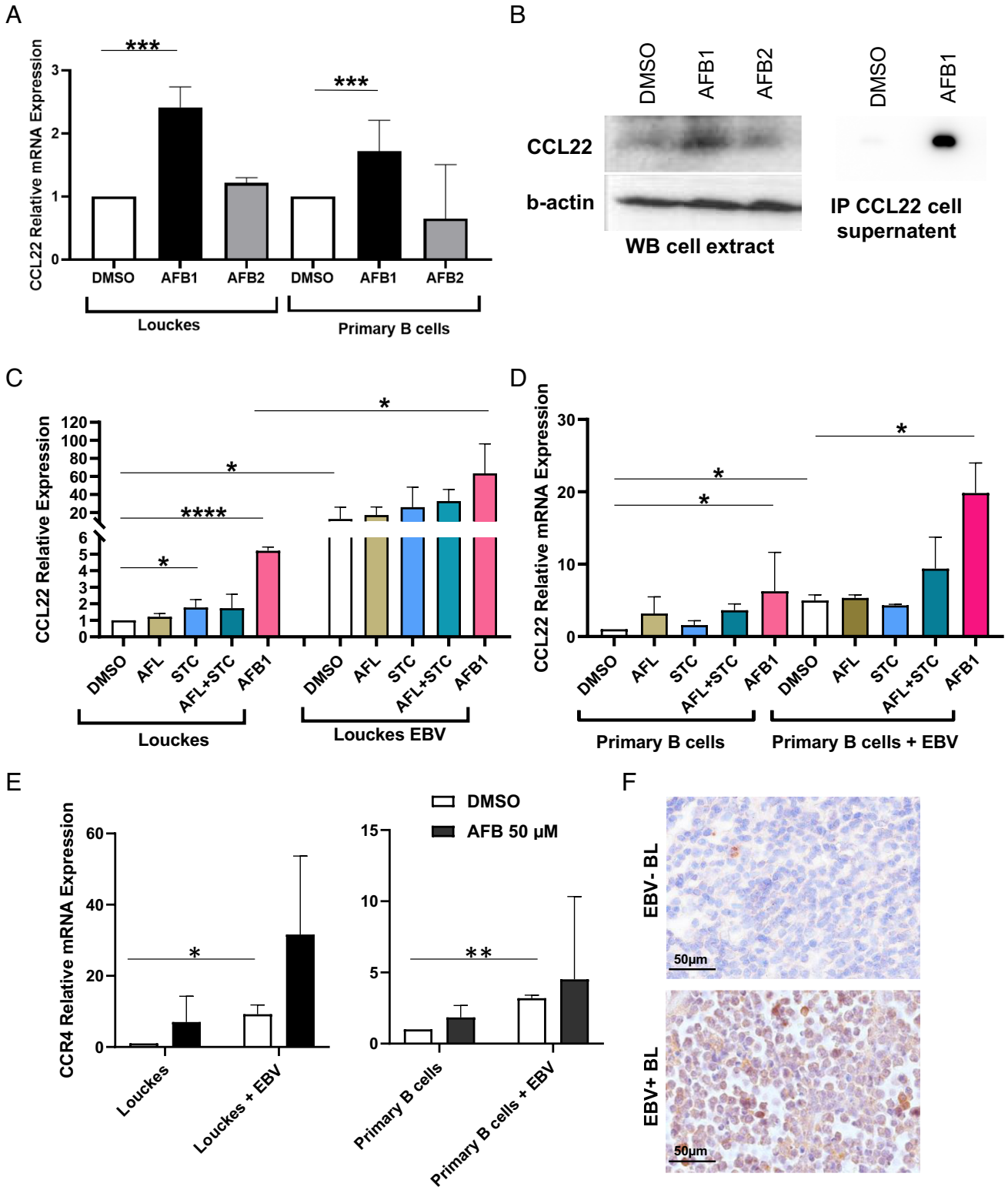

Fig. 1. Mycotoxins and EBV exposure increase *CCL22* expression. (*A*) *CCL22* relative mRNA expression levels in Louckes and primary B cells exposed to aflatoxin B1 (AFB1) 50 µM and B2 (AFB2) 50 µM. (*B*) CCL22 protein levels detected in presence and absence of aflatoxin exposure (50 µM) by Western Blot using total cell extract (*Left*) and immunoprecipitated (IP) CCL22 from cell supernatant (*Right*). (*C* and *D*) RT-qPCR quantification of *CCL22* mRNA levels in cells exposed to AFB1 (50 µM), aflatoxicol (AFL) at 25 µM, sterigmatocystin (STC) at 3.13 µM and combination of both (AFL+STC) for 48 h only or infected by EBV 24 h after treatment. (*E*) The RT-qPCR analyses of *CCR4* mRNA levels in Louckes and primary B cells exposed to AFB1 (50 µM) and EBV. DMSO was used as solvent control in all experiments. The histograms represent data mean ± SD and significance level calculated by ANOVA test (P *≤ 0.05, or P** ≤ 0.01, or P*** ≤ 0.001 or P**** ≤ 0.0001), n = 3. (*F*) Representative images of immunohistochemistry staining for CCL22 performed on EBV-positive (n = 8) and EBV-negative (n = 6) Burkitt Lymphomas.

CCL22 binding to its receptor on the membrane surface of B cells. Overall, our data show that both EBV and AFB1 stimulate the transcription of *CCL22*.

Further, to assess whether the increase in CCL22 detected following EBV infection is linked to EBV-associated BLs, we evaluated by immunohistochemistry CCL22 levels in EBV-positive

Downloaded from https://www.pnas.org by UNIVERSITEITSBIBLIOTHEEK GENT on June 6, 2024 from IP address 157.193.59.67.

(EBV$^+$) and EBV-negative (EBV$^-$) BL tumors. Our result revealed high CCL22 levels in EBV$^+$ BLs compared to EBV$^-$ tumors (Fig. 1*F* and *SI Appendix*, Fig. S1). This suggests that the increase in CCL22 levels induced by EBV and AFB1 exposure detected at early stages of B cell transformation might remain until BL tumor development and that CCL22 might play a functional role in EBV-associated BL tumorigenesis.

AFB1 and EBV Stimulate CCL22 Secretion via NF-kB Pathway Activation. To better understand the mechanism by which AFB1 and/or EBV promote the expression of *CCL22*, we evaluated whether AFB1 and EBV up-regulate *CCL22* via NF-kB pathway activation. This was motivated by the studies showing that EBV infection induces the NF-kB pathway through its latent gene LMP1 and that *CCL22* expression can be regulated by NF-kB (38). We treated Louckes cells with Bay11, an inhibitor of the Kinase IKKβ, the central regulator of NF-kB activation which phosphorylates IkBα, and assessed the expression of *CCL22* following AFB1 exposure and/or EBV infection. Treatment of Louckes cells with Bay11 at two different concentrations (1 or 10 μM) led to an almost complete abolition of induced *CCL22* expression by AFB1, EBV, and the synergy of both exposures (Fig. 2*A*) indicating that AFB1 and EBV favor *CCL22* mRNA expression by activating the NF-κB pathway. Similarly, transfection of cells with a specific siRNA directed against the p65 subunit of NF-kB inhibited the stimulation of *CCL22* expression by AFB1 and/or EBV (Fig. 2*B*). From this dataset, we conclude that exposure of B cells to AFB1 and/or EBV promotes the expression of *CCL22* by activating the NF-kB pathway.

EBV Latent Viral Proteins Play a Role in the Induction of *CCL22* Expression. To further dissect the viral mechanisms underpinning EBV-induced *CCL22* expression, we aimed to reveal the EBV viral genes involved in the regulation of *CCL22* overexpression. EBV infection was previously reported to induce *CCL22* expression by an LMP1-mediated mechanism, an event that may favor virus immune escape (38). To assess the role of LMP1 in enhancing *CCL22* expression, we infected primary B cells with EBV or a recombinant virus lacking LMP1 expression (EBV$_\Delta$LMP1) and analyzed the efficiency of infection by RT-PCR (Fig. 3*A*). At 48 h post infection, we collected the infected cells, validated the lack of expression of LMP1 (Fig. 3*A*), and confirmed that the efficiency of infection was similar in cells infected with EBV and EBV$_\Delta$LMP1 by evaluating the expression of *EBNA2* gene (Fig. 3*A*). As expected, EBV infection led to a strong expression of *CCL22* mRNA expression. Similarly, EBV$_\Delta$LMP1 infection was also able to induce a significantly high *CCL22* expression that is lower than the expression induced by the infection with the full EBV genome (Fig. 3*A*), suggesting that, in our experimental conditions, other viral proteins than LMP1 may also participate in inducing *CCL22* expression. To analyze the contribution of latent viral proteins in the activation of *CCL22* mRNA expression, we transfected Louckes cells with an expression vector for each viral protein, namely LMP2A, EBNA1, EBNA2, EBNA3A, EBNA3B, EBNA3C, and EBNALP. Following the transfection, we observed an increase in *CCL22* expression when vectors expressed LMP2A, EBNA1, EBNA2, EBNA3C, and EBNALP but not when the vectors expressed EBNA3A and EBNA3B. However, none of the

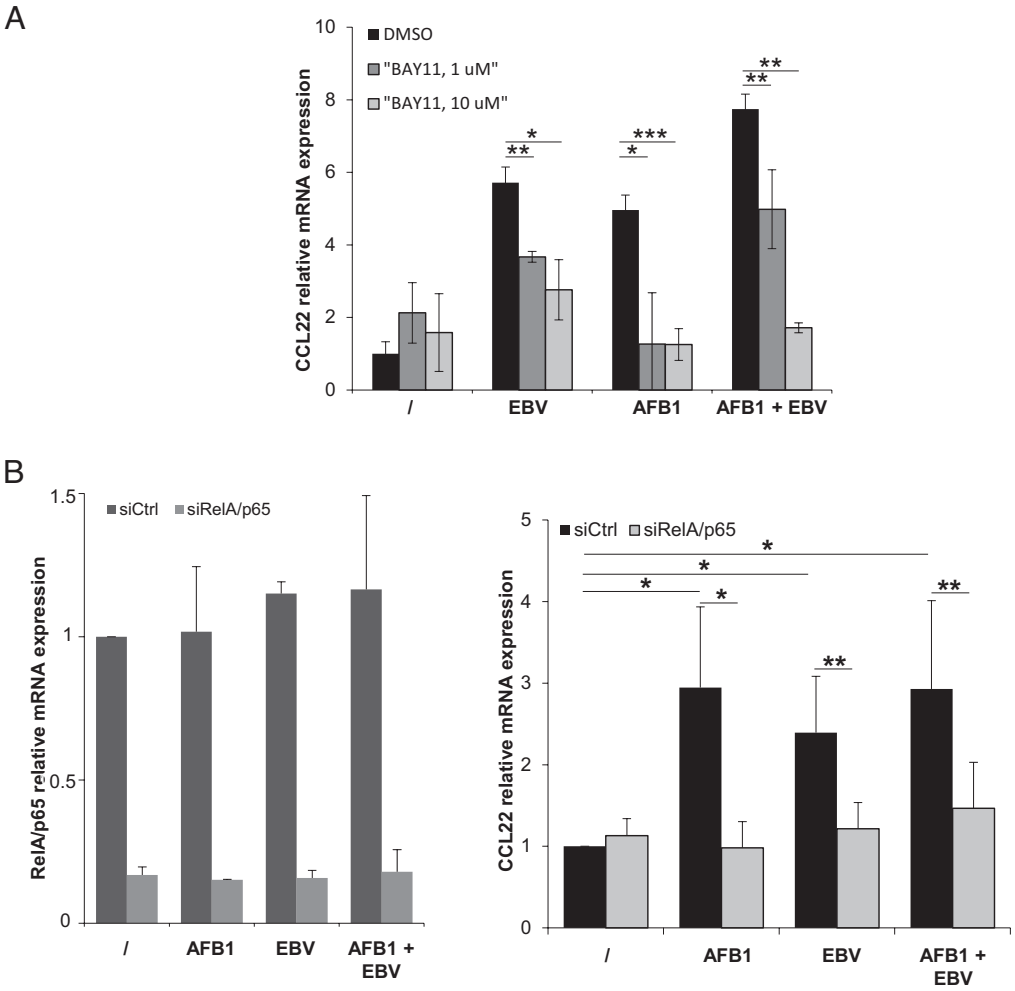

Fig. 2. AFB1 and EBV stimulate *CCL22* via the activation of NF-kB pathway. (*A*) RT-qPCR analysis of *CCL22* mRNA expression levels in Louckes cells exposed to NF-kB inhibitor (Bay11; used at 1 μM or 10 μM) under conditions of AFB1 treatment (50 μM) for 48 h, EBV for 24 h, or a combination of both EBV and AFB1 with nonexposed cells (*/*) as control. (*B*) RT-qPCR quantification of RelA/p65 (key subunit of NF-kB) mRNA expression levels in exposed Louckes cells as (*A*) and transfected with siRelA/p65 or scramble control (siCtrl) (*Left*). RT-qPCR relative quantification of *CCL22* mRNA in exposed cells transfected with siCtrl or siRelA/p65 (*Right*). Data are mean ± SD (n = 3) and significance level calculated by ANOVA test (*P** ≤ 0.05, or *P*** ≤ 0.01, or *P**** ≤ 0.001 or *P***** ≤ 0.0001).

Downloaded from https://www.pnas.org by UNIVERSITEITSBIBLIOTHEEK GENT on June 6, 2024 from IP address 157.193.59.67.

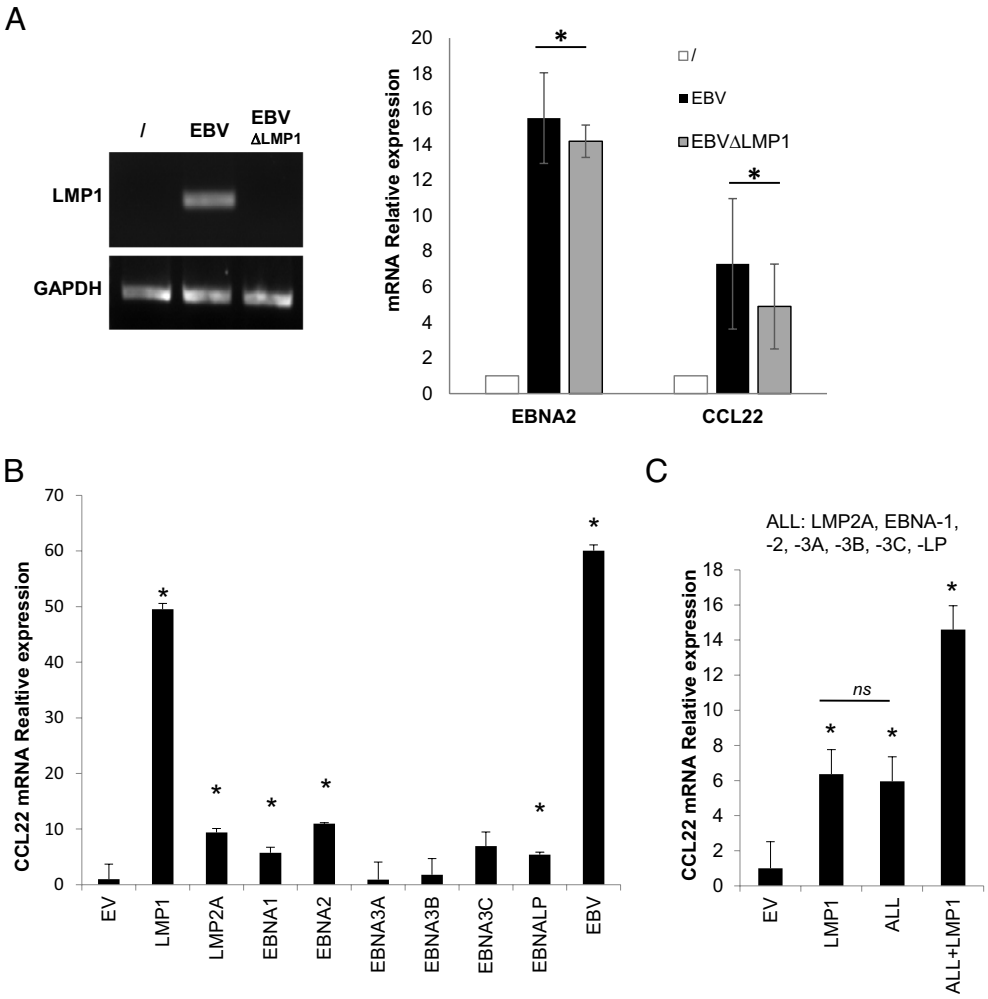

Fig. 3. EBV latent viral proteins play a role in induction of *CCL22* expression. (*A*) RT-PCR products of LMP1 and *GAPDH* amplification run on agarose gel confirming the efficiency of LMP1 deletion in EBV genome compared to empty vector control (*/*) used as negative control and EBV-infected Louckes cells as positive control (*Left*). mRNA quantification of EBNA2 (key EBV viral marker) and *CCL22* in Louckes cells infected with EBV or recombinant EBV (*Right*). (*B*) *CCL22* mRNA quantification by RT-qPCR of Louckes cells transfected with empty vector (EV), vector expressing individual EBV latent genes (LMP1, LMP2A, EBNA1, EBNA2, EBNA3A, EBNA3B, EBNA3C, and EBNALP) or infected with EBV. (*C*) RT-qPCR quantification of *CCL22* mRNA in Louckes cells transfected with either LMP1 expressing vector or with a mixture of vectors expressing all viral latent genes except LMP1 or with all viral latent genes including LMP1 or empty vector (EV) as control. Data are mean ± SD n = 3 and significance level calculated by ANOVA test for (*A*) and Student's *t* test for (*B*) and (*C*) ($P^* \leq 0.05$). ns: no significant difference between LMP1 and All viral latent genes.

transfected viral genes had an effect on *CCL22* induction similar to that of LMP1 (Fig. 3*B*). Interestingly, when transfected together, those latent genes were as effective as LMP1 and cooperated with it to activate *CCL22* expression to a higher level from when LMP1 is expressed alone (Fig. 3*C*). Further, we checked the expression of LMP1, EBNA2, and *CCL22* during EBV induced B cell immortalization. The latter is an in vitro model where B cells are infected with EBV for 21 d (40). In this model, EBV hijacks B cell maturation pathways leading to immortalization of the infected cells, with the generation of latently infected lymphoblastoid cell lines (LCL). This process of cell immortalization recapitulates aspects of B cell maturation in the germinal center, and LCL cells are an important model to study the biology of EBV infection and viral mechanisms potentially involved in malignant cell transformation. Our results show an increase in EBNA2 expression starting day 2 post-infection followed by an increase in LMP1 expression after day 2. However, *CCL22* expression appears to be highly expressed from day 2 onward (*SI Appendix*, Fig. S2) and slightly decreases at LCL stage when LMP1 is expressed at its highest level. Furthermore, in cells infected with recombinant virus lacking LMP1, *CCL22* expression still showed an increase during infection. These findings suggest that, in addition to the key role of LMP1, other EBV gene products may up-regulate *CCL22* expression.

CCL22 Enhances EBV Infection through Activation of PI3K Pathway. Because an increase in *CCL22* expression may affect the immune response and downstream internal pathways in B cell, it may impact subsequent infections of B cells including EBV. Hence, we sought to investigate whether increased *CCL22* expression could have an impact on EBV viral infection of B cells. To this end, we altered *CCL22* expression or CCL22 protein function in cells and assessed the level of EBV infection by viral DNA quantification and by flow cytometry. First, we blocked the interaction of CCL22 with its receptor CCR4 by adding a CCL22 neutralizing antibody (anti-CCL22 ab) to the culture medium. This led to a decrease in EBV infection efficiency of Louckes cells (Fig. 4*A*). Similarly, when we down-regulated *CCL22* expression by applying siRNA targeting *CCL22* in B cells followed by infection with EBV tagged with green fluorescent protein (GFP), we observed a decrease in the percentage of EBV GFP-positive B cells indicating a decrease in the infection efficiency of B cells (Fig. 4*B*). Consistent with these findings, an increase in EBV viral load was observed when a recombinant human CCL22 protein (RhCCL22) was introduced into the culture medium of B cells (Fig. 4*C*). An increase in EBV infection was also observed when siCCL22-treated cells were supplemented with RhCCL22 (Fig. 4*D*). Altogether, this indicates that an enhancement in *CCL22* expression results in an increase in EBV infection of B cells suggesting that the AFB1-induced CCL22 up-regulation might be underpinning an AFB1-associated increase in EBV infection. Therefore, we investigated whether AFB1 can increase the efficiency of EBV infection under conditions where *CCL22* overexpression is silenced. Our results showed that while levels of EBV infection in cells exposed to AFB1 were higher than in unexposed cells, they were similar to

Downloaded from https://www.pnas.org by UNIVERSITEITSBIBLIOTHEEK GENT on June 6, 2024 from IP address 157.193.59.67.

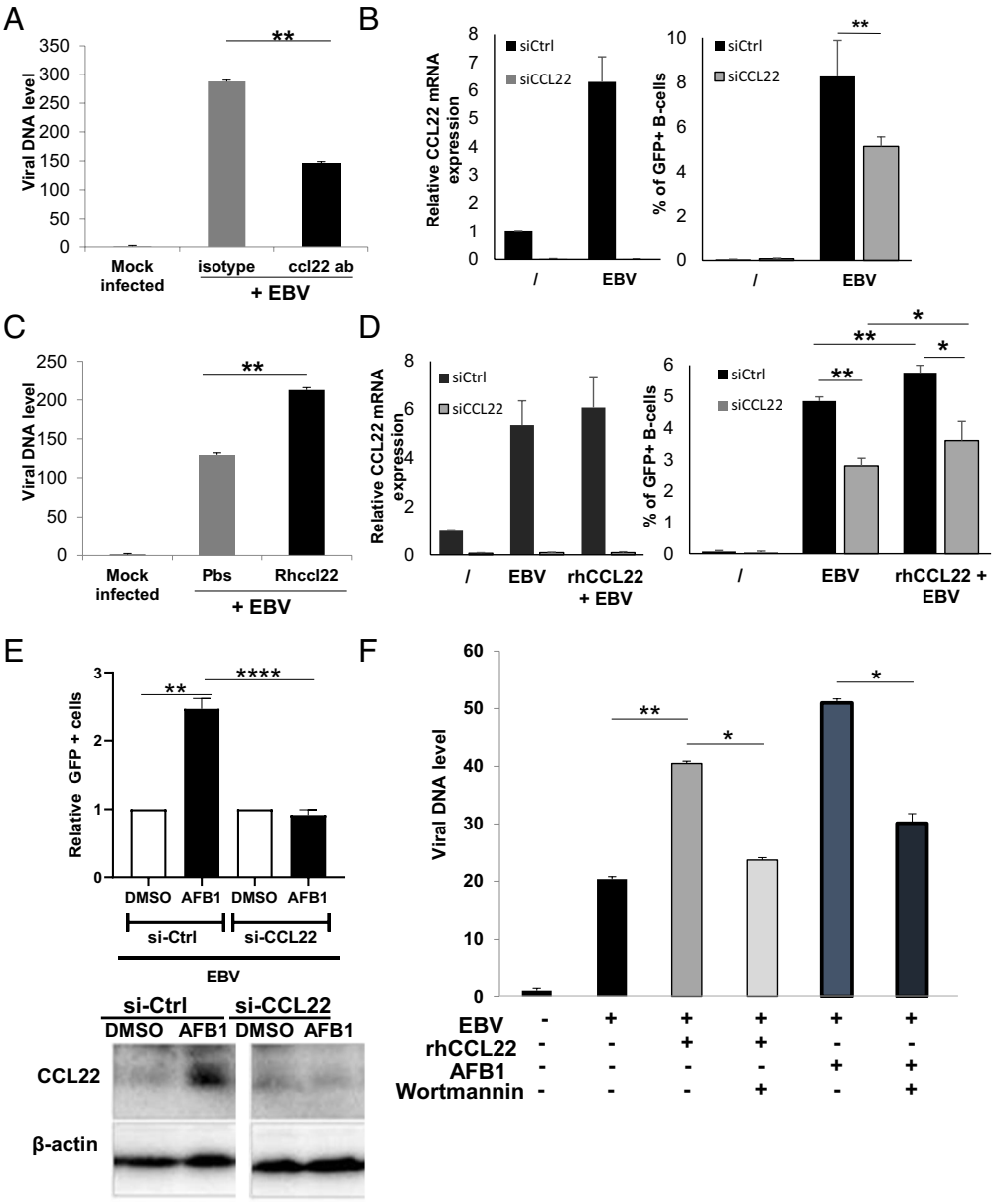

Fig. 4. CCL22 enhances EBV infection through activation of PI3K pathway. (*A*) qPCR quantification of viral DNA levels in EBV exposed primary B cells treated with CCL22 neutralizing antibody (CCL22 ab) or isotype antibody (isotype). (*B*) RT-qPCR analysis of *CCL22* gene silencing efficiency in EBV infected B cells (*Left*) and FACS analysis data indicating the percentage of green fluorescence protein EBV-positive B cells (%GFP+ B cells) in siCCL22 (siRNA against *CCL22*) versus siCtrl (scramble control) treated B cells infected with EBV (*Right*). (*C*) qPCR quantification of viral DNA levels in EBV exposed primary B cells treated with human recombinant CCL22 (RhCCL22) or phosphate buffered saline (Pbs). (*D*) Same as in (*B*). Mock infected cells were used as controls in all EBV infection experiments. (*E*) Viral quantification results by FACS in siCCL22 treated cells exposed to AFB1 50 μM (*Up*) and infected by EBV together with western blot results of CCL22 protein detection in treated cells (*Down*). (*F*) Viral DNA level by qPCR in exposed B cells treated with a PI3K inhibitor (Wortmannin) or untreated, exposure of cells was with either EBV, or EBV plus RhCCL22, or EBV plus AFB1. Dimethyl sulfoxide (DMSO) was used as solvent control in aflatoxins exposures. Histograms represent mean ± SD, n = 3, and significance level calculated by Student's *t* test ($P^* \leq 0.05$, or $P^{**} \leq 0.01$, or $P^{***} \leq 0.001$ or $P^{****} \leq 0.0001$).

unexposed cells when *CCL22* expression was down-regulated by siRNA (Fig. 4*E*). Together, these results indicate that AFB1 induction of *CCL22* plays a direct role in the efficiency of EBV infection by enhancing "de novo" infection or impacting the spread of the infection to other cells.

As the B cells exposed to AFB1 exhibit activated PI3K pathway (28), a cascade described to be activated by CCL22 (41), it was hypothesized that CCL22 may enhance EBV infection through activation of PI3K. Therefore, we evaluated the EBV infection efficacy in cells treated with AFB1 or RhCCL22 prior to infection by EBV in presence or absence of wortmannin, a PI3K pathway inhibitor. Our results revealed that wortmannin treatment resulted in a reduction in EBV infection efficiency even after the increase in CCL22 following addition of RhCCL22 on the cells or AFB1 exposure (Fig. 4*F*). These results support the role of CCL22 in promoting EBV infection through activation of the PI3K pathway.

Neutralizing CCL22 Limits EBV Infection in Humanized Mice. As our in vitro studies showed that CCL22 enhances EBV infection, we aimed to validate those data in an in vivo setting by evaluating the impact of neutralizing CCL22 function on the levels of EBV infection in a "humanized" mouse model. For that, we used non-obese diabetic/severe combined immunodeficient (NOD/LtSz-scid/IL2Rynull; NSG) mice reconstituted with human CD34+ hematopoietic stem cells (resulting in "humanized" mice; huNSG) that have been previously used to study EBV infection (28, 42, 43). To neutralize CCL22 function, we injected the huNSGs with a neutralizing anti-CCL22 antibody before and after infecting them with EBV (Fig. 5*A*). Our analysis of the levels of CCL22 in plasma using Luminex serology-based assay showed that mice treated with the neutralizing CCL22 antibody exhibit reduced level of CCL22 in plasma compared with untreated mice while, as expected, EBV infection in group B increased CCL22 levels (Fig. 5*B*). Interestingly, we observed lower levels of CCL22 in groups C and D compared to group A (Fig. 5*B*). The low levels of *CCL22* detected in group C injected with the neutralizing antibody compared to group A injected with the isotype that may be the result of a regulatory role of CCL22 on its own expression, validated the efficacy of the treatment. The impact of neutralizing CCL22 on EBV infection was then assessed by determining the viral load in the plasma of infected animals by Taqman qPCR

Downloaded from https://www.pnas.org by UNIVERSITEITSBIBLIOTHEEK GENT on June 6, 2024 from IP address 157.193.59.67.

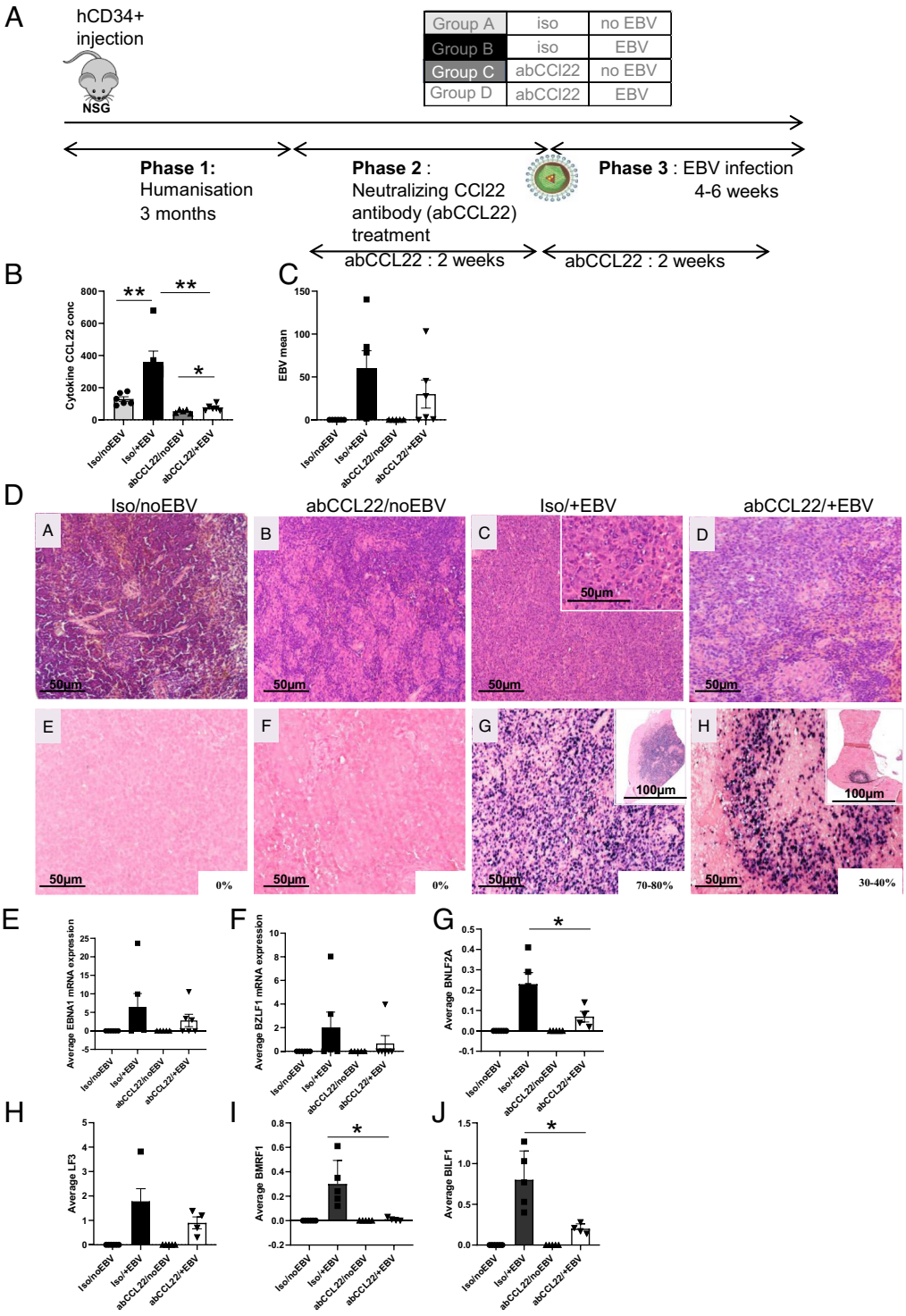

Fig. 5. Neutralizing CCL22 decreases EBV infection and expression of its latent and lytic genes in humanized mice tissues. (*A*) Schematic representation of mice intervention plan indicating the three phases composed of the humanization phase, neutralizing antibody administration phase (abCCL22 20 µg treatment per week for 4 wk) and EBV infection phase (0.5×10^5 particle). The mice were divided into four groups (5/6 mice per group) with treatment or infection as: (group-A) mice treated with isotype antibody with no EBV infection (Iso/noEBV), (group-B) mice treated with isotype antibody with EBV infection (Iso+EBV), (group-C) mice treated with CCL22 blocking antibody with no EBV infection (abCCL22/noEBV) and (group-D) mice treated with CCL22 blocking antibody with EBV infection (abCCL22+EBV), (*B*) Cytokine CCL22 concentration measured using Luminex serology-based assay in plasma samples from the four groups of humanized mice, (*C*) EBV mean levels measured in mice spleen DNA using Taqman PCR, (*D*) Hematoxylin and eosin (H&E) staining of mice spleen sections (*a*–*d*) and EBV-encoded RNA (EBER) in- situ hybridization (ISH) staining for EBV detection (*e*–*h*). Images shown are representative images of animals per group (n = 5 or 6 animals per group). Percentage of EBER-ISH positive cells per section is noted for (*e*–*h*), (*E*–*J*) Average viral gene (EBNA1 or BZLF1 or BNLF2A or LF3 or BILF1 or BMRF1) mRNA expression measured by qPCR on transcribed RNA from the spleen. Experiments represent n = 5 or 6 mean per group ± SEM and significance level calculated by Student's *t* test ($P^* \leq 0.05$ or $P^{**} \leq 0.01$, or $P^{****} \leq 0.0001$). NSG: NOD.Cg-Prkdc^{scid} Il2rg^{tm1Wjl}/SzJ mice.

(Fig. 5*C*). We have observed lower levels of EBV viral load in mice injected with the neutralizing antibody which validates the role of CCL22 in enhancing EBV infection.

Taking advantage of the collected tissues from the mice, we performed H&E staining and EBER in situ hybridization (EBER-ISH) analyses on spleen, lung, and liver tissues. The white pulp of the spleen showed a nodular pattern characterized by primary follicles in uninfected mice (Fig. 5 *D*, *a* and *e*). In addition, scattered epithelioid and non-necrotizing epithelioid granulomas were detected in uninfected mice treated with anti-CCL22 (Fig. 5 *D*, *b* and *f*). Interestingly, in mice infected with EBV, a diffuse lymphoid proliferation of large atypical cells that were EBER positive was found (Fig. 5 *D*, *c* and *g*), while in mice infected by EBV and treated with anti-CCL22 only a focal proliferation of these large atypical cells (EBER positive) surrounded by an inflammatory epithelioid granulomatous reaction was observed (Fig. 5 *D*, *d* and *h*). EBER-ISH analyses confirmed our in vitro results and further showed an impact of the neutralizing antibody on the levels and diffusion of EBV (Fig. 5 *D*, *e*–*h* and *SI Appendix*, Fig. S3). Finally, to determine whether the detected EBV in groups B and D is in lytic or latent phase, we assessed the mRNA expression levels of selected viral genes (latent gene e.g., EBNA1 and lytic gene e.g., BZLF1). As expected, the EBNA1 and BZLF1 mRNA expression levels were reduced in EBV infected

Downloaded from https://www.pnas.org by UNIVERSITEITSBIBLIOTHEEK GENT on June 6, 2024 from IP address 157.193.59.67.

mice treated with the CCL22 blocking antibody (Fig. 5 *E* and *F*) compared with mice treated with the control antibody. BNLF2A, LF3, BMRF1, and BILF1 all showed a lower expression level in mice injected with CCL22 neutralizing antibody (Fig. 5 *G–J*). These findings provide a solid validation of our in vitro findings showing that CCL22 enhances EBV infection.

Discussion

It has been hypothesized that chronic dietary intakes of mycotoxins, which are prevalent in the regions with high incidence of eBL in Africa, interact with oncogenic viruses to enhance the risk of developing juvenile carcinomas, although understanding the underlying mechanisms is limited. In the present study, we show that the mycotoxin AFB1 synergizes with EBV, via the NF-kB pathway, in the induction of the expression of the cytokine *CCL22* and its secretion. We also show that LMP1 as well as other viral latent gene products contribute to the EBV-induced *CCL22* expression. Interestingly, high *CCL22* expression, in part via the PI3K pathway, leads to an increase in the infection of B cells by EBV. Interestingly, we also reveal that in contrast to EBV-negative BLs, CCL22 is highly detected in EBV-positive BLs which supports a functional role for this cytokine in the process leading to B cell transformation by EBV and its co-factors in eBL.

The immunotoxicity of mycotoxins in immunosuppression has been widely discussed, but there are more and more reports on the inflammatory response induced by mycotoxins exposure. Those studies show that low doses of exposure to mycotoxins induce inflammations and high doses induce immunosuppression (44, 45). Mycotoxins have been proposed as toxic on innate and adaptive immunities of animals and cells. This toxicity includes affecting the proliferation, differentiation, or maturation of immune cells, cytokine production, antibody levels, and increasing the susceptibility to pathogens. Therefore, it is essential to further elucidate the pathogenic mechanism of specific mycotoxins. Here, we show that the exposure to the mycotoxin AFB1, but not to AFB2, results in an increased *CCL22* expression and CCL22 secretion by B cells. This increase was observed but to a lesser extent following STC and AFL exposure which could be due to the lack of a full AFB1 biosynthesis in vitro when cells are exposed to the precursor STC and/or to the lack of the other downstream metabolites of AFB1 in the case of AFL. An increase in CCL22 was previously observed in macrophages exposed to the trichothecene deoxynivalenol (DON) mycotoxin (46) suggesting a possible common response of immune cells exposed to different mycotoxins. The increase in *CCL22* following exposure to AFB1 is in line with previous reports showing expression changes of several genes involved in the immune response and related mechanisms and pathways in B cells exposed to AFB1 (29, 47) with an significant enrichment in pathways related to AKT, MAPK, mTOR, and PI3K signaling. Similar findings were obtained in AFB1-treated hepatocytes (48), suggesting that AFB1 can alter several signaling pathways that control cell's immune response, growth, and proliferation by inducing cytokine expression (49). Together, this provides unique insights into the mechanisms by which AFB1 exposure differentially modulates the cell-mediated immune responses and suggests the involvement of an inflammatory response upon repeated exposures.

In a similar manner to what has been observed following AFB1 exposure, EBV infection resulted in *CCL22* overexpression and its high secretion by B cells. Viral stimulation of *CCL22* has been reported following human cytomegalovirus (CMV), human T Cell leukemia virus type 1 (HTLV1), and hepatitis B virus (HBV) infection as a mechanism to escape immune surveillance and maintain local conditions favorable to their own growth and proliferation (31, 50, 51). Tumor cells secrete cytokines and chemokines, such as CCL28, CCL5/1, and CCL22 to create an immunosuppressive tumor microenvironment that prevents the recognition and destruction of tumor cells by effector T cells. CCL22 accumulation in solid tumors has also been shown to lead to CD4+ Treg lymphocytes infiltration in different tissues (33, 34, 52) that dampen antitumor immune responses. Moreover, high levels of circulating CCL22 are found in lymphomas (37, 53, 54), and in particular, it has been shown that EBV^+ tumors have amongst the highest levels of Treg of all human tumors, as well as having very high levels of CCL22 that promote the migration of Treg (37, 38, 55, 56). In addition to its well-recognized role in the control of the immune response, our results suggest that CCL22 could also be used to increase the infectivity of B cells by EBV. Previous reports described the increase of *CCL22* expression in several EBV^+ cancer cells (37) and in B cells infected with EBV. Those studies have shown that the EBV viral gene LMP1 induces the secretion of several cytokines including CCL22 in EBV-infected cells via activation of NF-κB. Our study extends those analyses and demonstrates that in addition to LMP1, other viral latent genes contribute to *CCL22* stimulation except EBNA 3A and 3B. The viral latent proteins seem to work in synergy as their combined effect on *CCL22* is observed to be equal to that of LMP1 alone. This suggests that LMP1 plays a major role in *CCL22* expression, but its effect is synergized and/or could be compensated by the action of other viral latent proteins. Previous studies have reported that LMP1 can cooperate with LMP2A to increase carcinogenesis (44–46), the increase of *CCL22* expression by LMP1 and LMP2A suggests a common mechanism, and that CCL22 could be involved in the cooperative mechanism of LMP1 and LMP2A.

Interestingly, we have revealed that both AFB1 and EBV have a synergistic impact on CCL22 induction further extending the mechanistic knowledge about the synergy of both exposures from our previous report showing their synergistic effect on TGFBI expression in B cells (29). Our results have also shown that the CCL22 upregulation by both exposures is largely due to the activation of the NF-κB pathway. This is consistent with reports showing that the NF-κB pathway can be triggered by EBV (57) and results into secretion of chemokines or cytokines such as CCL22 (38). However, while the induction of the NF-κB pathway by AFB1 has been described (58), to our knowledge, its impact on CCL22 secretion was not previously revealed. Whether NF-κB-induced *CCL22* overexpression is through its canonical or the noncanonical pathway for both exposures remains to be determined. Additionally, we show that both EBV and AFB1 stimulate the CCL22 B cells receptor CCR4. This may further lead to an increase in CCL22 internalization and induction of its downstream signals in B cells. Furthermore, this possibly enables CCL22 to sufficiently bind to its receptor, attract T helper 2 (Th2) cells and regulatory T cells (31, 33, 38), and inhibit T cytotoxic response that results to destruction of infected or abnormal cells. This may help EBV-infected B cells to evade immune surveillance by Th1 cells (31).

Remarkably, we have revealed that CCL22 overexpression generated by AFB1 and/or EBV in turn enhances EBV infection. These results provide further evidence and clarifications to the increase in EBV infection observed by us and others following mycotoxins exposures (28, 59). Understanding the impact as well as the upstream and downstream mechanisms of CCL22 induction could be of major interest to understand early mechanisms underpinning eBL. As infants from lymphoma belt regions are highly exposed to mycotoxins notably AFB1 early in life, this could result in a high CCL22 induction followed by an increase in EBV infection. The increase in EBV infection following up-regulation of CCL22 could be the result of an increase in the EBV uptake by cells by

Downloaded from https://www.pnas.org by UNIVERSITEITSBIBLIOTHEEK GENT on June 6, 2024 from IP address 157.193.59.67.

activating cellular pathway such as the PI3K pathway. In line with this notion, the PI3K pathway, although not studied in the context of EBV infection, has been described to be involved in enhancing the viral uptake of several viruses (60, 61). Activation of PI3K pathway is also expected to activate B cells and EBV lytic replicative cycle that might lead to oncogenesis by spreading the virus infected-naive B cells, transforming B cells and promoting oncogenesis (62). The involvement of PI3K in those mechanisms seems crucial because the inhibition of PI3K by Wortmannin blocked CCL22-induced EBV infection. Indeed, our previous studies identified PI3K pathway as one of the pathways enriched following AFB1 exposure (28). Moreover, viral proteins LMP1 and LMP2A have earlier been shown to activate this pathway (63). As the PI3K/Akt pathway is highly important in Burkitt lymphomagenesis in synergy with MYC (63), our results suggest an upstream role of CCL22 in eBL development. However, our in vitro and in vivo models mimic in many aspects the early stages of B cells infection, but they do not fully recapitulate eBL development. Therefore, our results reveal mechanisms that may be operating at early stages of B cell lymphomagenesis. Moreover, we show that CCL22 expression remains highly expressed in EBV-infected B cells until the formation of LCL cells. This process of cell immortalization recapitulates aspects of B cell maturation in the germinal center, and LCL cells are an important model to study the biology of EBV infection and viral mechanisms potentially involved in malignant cell transformation. Furthermore, our results revealed high CCL22 levels in EBV^+ eBLs compared to EBV^- tumors. Together, this suggests that CCL22 may contribute to eBL development although further in vitro and in vivo investigations are required to establish the role of EBV- and AFB1-induced CCL22 in B cell transformation and eBL development. These studies should also include monitoring the development of eBL tumors in mice that have been exposed to both EBV and AFB1 in the presence and absence of blocking Ab for CCL22.

Finally, we have shown that targeting CCL22 function limits EBV infection from spreading in vivo which may possibly prevent EBV-associated tumorigenesis. This effect seems to be mediated by an intense granulomatous reaction surrounding the focal proliferation of large $EBER^+$ atypical cells in mice infected by EBV and treated with anti-CCL22. Intriguingly, recent data using immunohistochemistry have shown that in case of Burkitt lymphoma with granulomatous reaction, there is a proinflammatory response and a prevalence of M1 macrophages, which can possibly explain the spontaneous regression observed in such cases (64). This proinflammatory response could involve the downregulation of CCL22. Indeed, several studies and preclinical and clinical approaches targeting directly or indirectly CCL22 have shown promising results in reducing immunosuppression and restoring an antitumor immune response (65–67). Our results are in line with those reports and propose that CCL22 could be used as a therapeutic target for the prevention of tumors associated with viral infection, notably in the context of EBV-induced tumorigenesis. Therefore, our current study provides valuable insights into pathways that can be targeted in cancer drug development especially immunotherapeutic or chemotherapeutic drugs. It also provides the foundation for future studies in the fields of epidemiology and immunomodulatory studies specifically pertaining to the investigation of carcinogenesis and the identification of risk factors.

Materials and Methods

Cell Culture. All cells were cultured in RPMI 1640 media (31870074; Thermo Fisher Scientific) supplemented with 10% Fetal bovine serum (S68028-0230; ABCYS EUROBIO), 1% Penicillin/Streptomycin 100×: U/mL 100/100 mg/mL (15140122; Thermo Fisher Scientific), 1 mM Sodium pyruvate (11360039; Life Technologies) 1%, 2 mM L-glutamine 100× (25030024; Thermo Fisher Scientific) 1% and incubated at 37 °C, 95% humidity, and 5% CO_2 with every 48 h passaging. Louckes and Raji cells were obtained from International Agency for Research on Cancer (IARC) biobank while primary B cells were generated from whole blood obtained from three different anonymous volunteer donors (authorization number: Codecho DC-2020-4217); the blood was purified using RosetteSep human B cell enrichment kit (15064; Stem Cell Technologies) based on manufacturers protocol.

Mycotoxin Exposure and EBV Infection of the Cells. Prior to mycotoxins exposures to the cells, a cytotoxicity test was done using MTS assay (G3580; Promega, CellTiter96 Aqueous one solution cell proliferation assay) based on the manufacturer's instructions to determine the right concentration of mycotoxins to use. Several concentrations of the mycotoxins were tested at different time points (24 h, 48 h, and 72 h). Concentrations with viability above 80% (O.D fold control above 0.8) were considered for experimental exposures (*SI Appendix*, Fig. S4). In the experimental setup, the cells were exposed to the selected concentrations of each of the mycotoxins: AFB1 at 50 μM (A6636; Sigma) or AFL at 25 μM (29611-03-8; Fermentek) or STC at 3.13 μM (S3255; Sigma Aldrich) or an equal combined exposure of AFL and STC in the concentrations stated above with dimethyl sulfoxide (DMSO) (D2650; Sigma Aldrich) used as the solvent control. AFB2 (A9887; Sigma) was used in the experiment in similar concentrations as AFB1 (47, 68). The cells were exposed to the mycotoxins for 48 h with EBV (B95-8 strain; particles produced from culturing HEK293EBVgfp cells) infection done in between mycotoxins exposures (EBV infection done after 24 h exposure). EBV infection was done as previously described by Lopez-Serra and Esteller (69) for 24 h incubation (5% CO_2, 37° C, and 95% humidity) or kept without EBV infection for 24 h. The viable cell number and percentages were again checked after the exposure and infection incubation period just before harvesting of the cells.

Extraction of DNA and RNA. The extraction of DNA and RNA from Louckes cells was done using AllPrep DNA/RNA minikit (Qiagen) that allows to extract DNA and RNA from the same sample while extraction of DNA and RNA from primary B cells was done using NucleoSpin Genomic DNA extraction kit (Macherey Nagel Rev 01, France) and NucleoSpin RNA Plus XS (Macherey Nagel Rev 16, France) respectively. All extractions and purification of the DNA or RNA were done based on the manufacturer's protocol. The extracted RNA or DNA were quantified using the NanoDrop spectrophotometer (BioRad) or Qubit (Invitrogen), then DNA was stored at −20 °C while RNA was stored at −80 °C until use.

qRT-PCR. Reverse transcription was done using 500 ng of RNA using the Reverse Transcription protocol Revert Aid H Minus First Strand cDNA synthesis kit (K1631; ThermoFisher Scientific). Quantitative PCR was then performed in duplicates using cDNAs, specific primers from Qiagen (Table 1), and master mix reagent from BioRad [Sso Advanced universal SYBR Supermix (10 × 1 mL) 1725272; BioRad]. The average levels of three house-keeping genes (Actin, GAPDH, and Beta 2 globulin) or Beta 2 microglobulin (μglobulin) only run together with the samples on the same plate setup was used for normalization. This was done to check the expression of genes of interest, e.g., CCL22 in exposure or treatment with mycotoxins or EBV.

Quantification of viral infection in the cells was done using TaqMan PCR (ABI Prism sequence detection system 7900HT; Applied Biosystems); primers and probes are listed in Table 1. Master mix Absolute QPCR Rox Mix (ref: CM-205A; Life Technologies) was used. Specific standards were prepared in triplicates using Raji EBV positive cell line DNA as reference for virus per cell number and quantification samples done in duplicates. The protocol described previously by Accardi et al. (28) was used.

Briefly, the PCR reaction was performed using 100 to 150 ng of DNA, 1 × ddPCR Supermix for Probes (BioRad), 0.30 μM of each primer, and 0.6 μM of the probe in a total volume of 22 μL. After droplet generation using the QX200TM Droplet Generator instrument (BioRad), the generated microdroplets were put into a 96-well plate for amplification. Cycling conditions included preheating at 95 °C for 10 min followed by 40 cycles of denaturation at 94 °C for 30 s, annealing at 58 to 60 °C for 60 s, and final heating at 98 °C for 10 min. Then, the PCR plate was transferred to a QX100 droplet reader (BioRad), and fluorescence amplitude data were obtained by QuantaSoft software (BioRad). The absolute copy number of each viral assay was calculated by Bio-Rad software and shown as the number of copies/μL. All primers and probes sequences are listed in Table 1.

Downloaded from https://www.pnas.org by UNIVERSITEITSBIBLIOTHEEK GENT on June 6, 2024 from IP address 157.193.59.67.

Table 1. Primers used for qPCR, TaqMan PCR, and ddPCR

Gene	Forward primer	Reverse primer
Primers used for qPCR		
Beta 2 μglobulin	CAGCCCAAGATAGTTAAGTG	ACAAGCTTTGAGTGCAAGAG
CCL22	ACTGCACTCCTGGTTGTCCT	CGGCACAGTCTCCTTATCCC
CCR4	TAATATTGCAAGGCAAAGACTATTCC	GCGATTTACTCCATCAGCCAGTA
LMP1	TGAACACCACCACGATGACT	GTGCGCCTAGGTTTTGAGAG
LMP2A	CCAGTCCAGTCACTCATAACG	CCTACATAAGCCTCTCACACT
Beta 2 globulin	CTCACGTCATCCAGCAGAGA	CGGCAGGCATACTCATCTTT
EBNA1	AAAGCATCGTGGTCAAGGAG	CAGTTCCTCGCCTTAGGTTG
EBNA2	ATATGACGTCGGGCATGGAC	GGTGACAAAATGGTGGGTGC
GAPDH	GCCAAAAGGGTCATCATC	TGCCAGTGAGCTTCCCGTTC
BZLF1	AATGCCGGGCCAAGTTTAAGCAAC	TGGGCACATCTGCTTCAACAGGA
Actin	CTGGGAGTGGGTGGAGGC	TCAACTGGTCTCAAGTCAGTG
Primers and probe for Taqman		
EBV W1	GCAGCCGCCCAGTCTCT	
EBV W2	ACAGACAGTGCACAGGAGCCT	
EBV probe	AAAAGCTGGCGCCCTTGCCTG 5′-FAM 3-TAMRA, 100 μM	
Beta globin	GTGCACCTGACTCCTGAGGAGA	CCTTGATACCAACCTGCCCAG
Beta globin probe	AAG GTGAACGTGGATGAAGTTGG 5′-HEX 3-TAMRA, 100 μM	
Primers and probes for digital PCR (ddPCR)		
BILF1	BILF1 F: TGCCTTTTGACCCAGAACATG	
	BILF1 R: CAACGCCATACCCAAGTGAGT	
	BILF1 probe: TACGGAGCACATCAGGCCCAAGAACA	
LF3	LF3 F: AGGGCTGGGTCCTGAGA	
	LF3 R: ACACGTGATGTAAGTTTAGCCAGTT	
	LF3 probe: GACTTTCGGGGCATT	
BNLF2A	BNLF2A F: TGGAGCGTGCTTTGCTAGAG	
	BNLF2A R: GGCCTGGTCTCCGTAGAAGAG	
	BNLF2A probe: CCTCTGCCTGCGGCCTGCC	
BMRF1	BMRF1 F: GAGGAACGAGCAGATGATTGG	
	BMRF1 R: TGCCCACTTCTGCAACGA	
	BMRF1 probe: TGCTGTTGATGCCCAAGACGGCTT	

Induction of Gene Expression Silencing Using siRNA. Gene silencing of *CCL22* and p65 was performed using *CCL22* and p65 (human) unique 27mer siRNA duplexes; CCL22HSS109578 and IKBKBVHS40301 Invitrogen life technology. Louckes cells (5×10^6) were transfected with the siRNA (final concentration, 250 nM) by electroporation using the Neon Transfection System (10 μL tips, pulse voltage 1,350 V, pulse width, 40 ms). At 48 h post-transfection, cells were collected and processed for RNA extraction. The levels of silencing were evaluated by RT-qPCR using gene-specific primers for *CCL22* and p65. Primers are indicated in Table 1.

Immunoblotting. This was done as previously described by Vargas Ayala et al. (70). Briefly, the entire cell lysate extracts or cell supernatant (collected after cells centrifugation) were obtained using lysis buffer (Laemmli sample buffer; Biorad No. 161073EDU) and fractionated by sodium dodecyl sulfate polyacrylamide gel electrophoresis (SDS-PAGE) and processed for immunoblotting using standard techniques. CCL22 antibody (Human CCL22/MDC; MAB336-500 R&D System) was used. Images were produced using a ChemiDoc XRS imaging system (Bio-Rad).

FACS Analysis. The percentage of EBV-GFP-positive B cells was assessed by fluorescence-activated cell sorting (FACS; FACSCanto system II; Becton, Dickinson) 24 to 48 h post EBV infection of Louckes cells. Briefly, cells were harvested, washed with PBS, and fixed with 1% paraformaldehyde for 15 min at room temperature. Cells were then washed with PBS and analyzed by flow cytometry to determine the percentage of EBV-GFP-positive B cells.

FACS analysis was also used to determine the level of humanization of the mice; percentages of average cells positive for the human leucocyte marker CD45, the human B cells marker CD19, and human T cells CD3 was measured (average of CD19 positive cells was 60% and CD3/CD45 was 37%).

In Vivo Mice Intervention. Non-obese diabetic/immunodeficient mice (NOD/LtSz-scid/IL2Rnull; Charles River Laboratories) reconstituted with human CD34+ hematopoietic stem cells (huNSG) from anonymous donors were used. The experiments were conducted in accordance with the set guidelines for animal care and use (ACUC). The experimental design and protocols were approved by the local ethics committee (approval number 13323-2017113013563410). The protocol used previously by Accardi et al. (22) was modified to be adapted to this study. Briefly, CCL22 function was neutralized by treating the mice with a neutralizing anti-CCL22 antibody (abCCL22; mouse IgG2B anti human ccl22 R&D system clone 57226 lot BIK0316091) at 20 μg per injection per mouse every week. Anti-CCL22 antibody was used for 2 wk before and after EBV infection (total 4 wk of abCCL22 administration) see Fig. 5*A*. EBV infection continued for 4 to 6 wk after which samples were collected. The effective concentration of abCCL22 and administration period was selected based on the outcome of a prior pilot study carried out to assess the best protocol to efficiently inactivate circulating CCL22 by injecting a neutralizing antibody: best injection route, number of injections per week and low toxicity were considered. The amounts of the neutralizing antibody abCCL22 tested in the pilot study were 5 μg, 10 μg, and 20 μg with administration

Downloaded from https://www.pnas.org by UNIVERSITEITSBIBLIOTHEEK GENT on June 6, 2024 from IP address 157.193.59.67.

period through intraperitoneal injection of once per week or twice per week considered. The results indicated that the use of 20 μg abCCL22 injections once per week for a period of 4 wk was effective in neutralizing CCL22 secretion in the humanized mice. Then, the EBV infection efficacy was evaluated through the determination of the viral titer in the blood of the infected mice and by measuring the spread of the infection to secondary lymphoid organs (e.g., spleen). A total of 24 humanized mice (housed at animal facility at ENS-PBES located in Lyon, France) were divided into 4 groups of six mice per group. All animals included in the study had similar average percentages of cells positive for the human leucocyte marker CD45 (hCD45+), the human B cells marker CD19 (hCD19+), and human T cells CD3 (hCD3+). The mice of different groups were treated as shown in Fig. 5*A*: (group-A) mice treated with isotype antibody without EBV infection, (group-B) mice treated with isotype antibody and infected with EBV, (group-C) mice treated with CCL22 neutralizing antibody (abCCL22) without EBV infection, and (group-D) mice treated with abCCL22 and infected with EBV. In groups B and D, 0.5×10^5 EBV particles were injected intraperitoneally. In groups C and D, 20 μg abCCL22 was administrated intraperitoneally once per week (3 wk before EBV infection and 2 wk after). At the end of the study (around 6 wk after EBV infection and 4 wk after the last abCCL22 injection administrated to stop the effect of abCCL22), mice were sacrificed, and blood and organs e.g., spleen, liver and lungs were collected and processed as previously described in Accardi et al. (22). Samples were then analyzed for viral load using Taqman qPCR, CCL22 cytokine quantification by Luminex assay, viral gene expression by RT-qPCR, and digital PCR, and the tissues were histologically processed and stained for EBER (see Histological and EBER-ISH staining section).

Luminex-Based Serology Assay. Plasma samples obtained from mice were analyzed using Luminex-based serology standard protocol for cytokine MDC quantification (HCYP4MAG-64 K; Milliplex Merck) done based on the manufacturer's protocol. Blood was collected from mice after being sacrificed through venipuncture and placed in EDTA anticoagulant-containing tubes. The blood was afterward centrifuged down at 1,000 rpm for 10 min to obtain plasma. A plasma volume of 25 μL was used for the analyses. Biotin binding protein that is fluorescently labeled, streptavidin-phycoerythrin was used for detection. A set of serial dilutions of a standard provided by the kit were used to generate a standard curve from which sample concentrations were read out.

Histological and EBER-ISH Staining. Formalin-fixed paraffin embedded tissue (FFPE) samples were stained with hematoxylin-eosin (H&E) for histological examinations. The results of the staining were analyzed by two pathologists (S.L. and L.L.) in a blinded manner. EBV was detected by in situ hybridization (ISH) with EBV-encoded small RNA (EBER) probes. The assay was performed on a Ventana Benchmark ULTRA instrument using ISH iView Blue Detection Kit according to the manufacturer's instructions (Ventana Medical Systems). A control slide, prepared from a paraffin-embedded tissue block containing metastatic nasopharyngeal carcinoma in a lymph node accompanied each hybridization run.

Immunohistochemistry Analysis of CCL22. EBV-positive (n = 8) and EBV-negative (n = 6) Burkitt Lymphomas from Nairobi Kenya were used for this analysis (ethical approval number from local committees: P668/08/2021). Immunohistochemistry staining was performed on FFPE 4-μm-thick sections by an automated staining system (Ventana BenchMark Ultra; Roche Diagnostics) using anti-CCL22 (EPR1362, Abcam: 1:50 dilution) (70). An UltraView universal detection kit (Ventana) using a horseradish peroxidase multimer and DAB (as the chromogen) was used for detecting the staining signal. FFPE sections from colon cancer tissues were used as controls.

Statistical Analysis. Data were analyzed by two-way ANOVA (Fig. 1 *C–E*) and one-way ANOVA (Figs. 1*A*, 2 *A* and *B*, and 3*A*) followed by multiple comparisons or Student's *t* test (Figs. 3 *B* and *C*, 4, and 5). Differences of P value ≤ 0.05 were considered significant. P values are indicated for each result with SD or SEM.

Disclaimer

Where authors are identified as personnel of the International Agency for Research on Cancer/World Health Organization, the authors alone are responsible for the views expressed in this article and they do not necessarily represent the decisions, policy, or views of the International Agency for Research on Cancer/World Health Organization.

Data, Materials, and Software Availability. All study data are included in the article and/or *SI Appendix*.

ACKNOWLEDGMENTS. We acknowledge the contribution of the Etablissement Français du Sang Auvergne-Rhône-Alpes by providing access to blood donations. Many thanks to our funders for financially supporting this research, the funders include; FWO Belgium (G085921N, to Z.H., S.D.S., M.D.B., and R.A.G.), Children with Cancer UK (CwC UK, PP201910-33 to G.A.O.), and Grand Challenges Exploration Grant from the Bill and Melinda Gates Foundation (Grant Number: OPP1061062 to Z.H.), INSERM grant PlanCancer ITMO to H.G. and Z.H., and PEDIAC "origines des cancers pédiatriques" grant from the national cancer institute (INCA France; grant number: INCA_15670 to R.K. and Z.H.), and the European Union's Horizon 2020 research and innovation program under the Marie Skłodowska-Curie grant agreement No 896422 to L.M. University of Limerick. Thanks also to all members of the Epigenomics and Mechanisms Branch at IARC especially to Cyrille Cuenin, Elizabeth page, Sandrine Chopin, and Aurelie Sallé. We are also grateful to Amelie Chabrier for the technical support and IARC fellowship team. We thank the platform animal facility (PBES, Plateau de Biologie Experimental de la Souris, UMS3444/CNRS, US8/Inserm, ENS de Lyon, UCBL), and Véronique Pierre for her technical help in handling mice.

Author affiliations: [a]Centre International de Recherche en Infectiologie, University Claude Bernard Lyon I, INSERM U1111, CNRS UMR5308, Ecole Normale Supérieure, Lyon 69366 Cedex 07, France; [b]Epigenomics and Mechanisms Branch, International Agency for Research on Cancer, World Health Organization, Lyon 69366 Cedex 07, France; [c]Limerick Digital Cancer Research Centre, Health Research Institute, Bernal Institute and School of Medicine, University of Limerick, Limerick V94 T9PX, Ireland; [d]Department of Medical Biotechnology, Section of Pathology, University of Siena, Siena 53100, Italy; [e]Centre of Excellence in Mycotoxicology and Public Health, Department of Bioanalysis, Faculty of Pharmaceutical Sciences, Ghent University, Ghent 9000, Belgium; and [f]Department of Biotechnology and Food Technology, Faculty of Science, University of Johannesburg, Gauteng 2028, South Africa

Author contributions: M.A.M., E.M., R.A., Z.H., H.G., and R.K. designed research; M.A.M., G.A.O., L.M., F. Manara, F. Mure, F.F., A.J., D.F., E.M., T.O., F.-L.C., R.A., H.G., and R.K. performed research; L.M., T.G., D.F., L.L., P.M., E.M., T.O., F.-L.C., S.L., R.A., Z.H., H.G., and R.K. contributed resources/reagents/analytical tools; M.A.M., G.A.O., L.M., F. Manara, F. Mure, F.F., T.G., T.M.M., L.L., P.M., E.M., T.O., M.D.B., S.D.S., S.L., R.A., Z.H., H.G., and R.K. analyzed data; M.D.B., and S.D.S. contributed with their expertise in mycotoxins; F.F., and F.-L.C. contributed to the mice experiments; and G.A.O., Z.H., H.G., and R.K. wrote the paper.

The authors declare no competing interest.

This article is a PNAS Direct Submission. E.C. is a guest editor invited by the Editorial Board.

Copyright © 2024 the Author(s). Published by PNAS. This article is distributed under Creative Commons Attribution-NonCommercial-NoDerivatives License 4.0 (CC BY-NC-ND).

1. D. A. Thorley-Lawson, M. J. Allday, The curious case of the tumour virus: 50 years of Burkitt's lymphoma. *Nat. Rev. Microbiol.* **6**, 913–924 (2008).
2. G. Pannone *et al.*, The role of EBV in the pathogenesis of Burkitt's Lymphoma: An Italian hospital based survey. *Infect. Agents Cancer* **9**, 34 (2014).
3. R. Ayee *et al.*, Epstein Barr virus associated lymphomas and epithelia cancers in humans. *J. Cancer* **11**, 1737–1750 (2020).
4. M.-R. Chen, Epstein-Barr virus, the immune system, and associated diseases. *Front. Microbiol.* **2**, 5 (2011).
5. M. K. Smatti *et al.*, Epstein-Barr virus epidemiology, serology, and genetic variability of LMP-1 oncogene among healthy population: An update. *Front. Oncol.* **8**, 211 (2018).
6. O. L. Hatton *et al.*, The interplay between Epstein-Barr virus and B lymphocytes: Implications for infection, immunity, and disease. *Immunol. Res.* **58**, 268–276 (2014).
7. P. Mrozek-Gorska *et al.*, Epstein–Barr virus reprograms human B lymphocytes immediately in the prelatent phase of infection. *Proc. Natl. Acad. Sci. U.S.A.* **116**, 16046–16055 (2019).
8. C. Münz, Latency and lytic replication in Epstein-Barr virus-associated oncogenesis. *Nat. Rev. Microbiol.* **17**, 691–700 (2019).
9. S. C. Kenney, J. E. Mertz, Regulation of the latent-lytic switch in Epstein-Barr virus. *Semin. Cancer Biol.* **26**, 60–68 (2014).
10. C. C. Sun, D. A. Thorley-Lawson, Plasma cell-specific transcription factor XBP-1s binds to and transactivates the Epstein-Barr virus BZLF1 promoter. *J. Virol.* **81**, 13566–13577 (2007).
11. A. Saha, E. S. Robertson, Mechanisms of B-cell oncogenesis induced by Epstein-Barr virus. *J. Virol.* **93**, e00238-19 (2019).
12. G. K. Hong *et al.*, Epstein-Barr virus lytic infection contributes to lymphoproliferative disease in a SCID mouse model. *J. Virol.* **79**, 13993–14003 (2005).

Downloaded from https://www.pnas.org by UNIVERSITEITSBIBLIOTHEEK GENT on June 6, 2024 from IP address 157.193.59.67.

13. C. B. Whitehurst *et al.*, Knockout of Epstein-Barr virus BPLF1 retards B-cell transformation and lymphoma formation in humanized mice. *mBio* **6**, e01574–e01615 (2015).
14. F. Aguayo *et al.*, Interplay between Epstein-Barr virus infection and environmental xenobiotic exposure in cancer. *Infect. Agent Cancer* **16**, 50 (2021).
15. I. I. Daud *et al.*, Plasmodium falciparum Infection is associated with Epstein-Barr virus reactivation in pregnant women living in malaria holoendemic area of Western Kenya. *Maternal Child Health J.* **19**, 606–614 (2015).
16. A. Chêne *et al.*, A molecular link between malaria and Epstein-Barr virus reactivation. *PLOS Pathogens* **3**, e80 (2007).
17. I. Magrath, Denis Burkitt and the African lymphoma. *Ecancermedicalscience* **3**, 159–159 (2009).
18. J. D. Groopman, T. W. Kensler, C. P. Wild, Protective interventions to prevent aflatoxin-induced carcinogenesis in developing countries. *Annu. Rev. Public Health* **29**, 187–203 (2008).
19. A. James, V. L. Zikankuba, Mycotoxins contamination in maize alarms food safety in sub-Sahara Africa. *Food Control* **90**, 372–381 (2018).
20. H. Hernandez-Vargas *et al.*, Exposure to aflatoxin B1 in utero is associated with DNA methylation in white blood cells of infants in The Gambia. *Int. J. Epidemiol.* **44**, 1238–1248 (2015).
21. A. Ghantous *et al.*, Aflatoxin exposure during early life is associated with differential DNA methylation in two-year-old gambian children. *Int. J. Mol. Sci.* **22**, 8967 (2021).
22. X. Lai *et al.*, Potential for aflatoxin B1 and B2 production by Aspergillus flavus strains isolated from rice samples. *Saudi J. Biol. Sci.* **22**, 176–180 (2015).
23. W. Iram *et al.*, Structural analysis and biological toxicity of Aflatoxins B1 and B2 degradation products following detoxification by ocimum basilicum and cassia fistula aqueous extracts. *Front Microbiol.* **7**, 1105 (2016).
24. M. G. Theumer *et al.*, Genotoxicity of aflatoxins and their precursors in human cells. *Toxicol. Lett.* **287**, 100–107 (2018).
25. C. Al-Ayoubi *et al.*, Metabolism of versicolorin A, a genotoxic precursor of aflatoxin B1: Characterization of metabolites using in vitro production of standards. *Food Chem. Toxicol.* **167**, 113272 (2022).
26. I. Caceres *et al.*, Aflatoxin biosynthesis and genetic regulation: A review. *Toxins (Basel)* **12**, 150 (2020).
27. A. S. Hamid *et al.*, Aflatoxin B1-induced hepatocellular carcinoma in developing countries: Geographical distribution, mechanism of action and prevention. *Oncol. Lett.* **5**, 1087–1092 (2013).
28. R. Accardi *et al.*, The mycotoxin aflatoxin B1 stimulates Epstein-Barr virus-induced B-cell transformation in in vitro and in vivo experimental models. *Carcinogenesis* **36**, 1440–1451 (2015).
29. F. Manara *et al.*, Epigenetic alteration of the cancer-related gene TGFBI in B cells infected with Epstein-Barr virus and exposed to Aflatoxin B1: Potential role in Burkitt lymphoma development. *Cancers* **14**, 1284 (2022).
30. B. Liu *et al.*, Affinity-coupled CCL22 promotes positive selection in germinal centres. *Nature* **592**, 133–137 (2021).
31. E. Poole *et al.*, NF-kappaB-mediated activation of the chemokine CCL22 by the product of the human cytomegalovirus gene UL144 escapes regulation by viral IE86. *J. Virol.* **82**, 4250–4256 (2008).
32. J. Korbecki *et al.*, CC chemokines in a tumor: A review of pro-cancer and anti-cancer properties of the ligands of receptors CCR1, CCR2, CCR3, and CCR4. *Int. J. Mol. Sci.* **21**, 1–29 (2020).
33. Y. Q. Li *et al.*, Tumor secretion of CCL22 activates intratumoral Treg infiltration and is independent prognostic predictor of breast cancer. *PLoS One* **8**, e76379 (2013).
34. J. Klarquist *et al.*, Ccl22 diverts T regulatory cells and controls the growth of melanoma. *Cancer Res.* **76**, 6230–6240 (2016).
35. T. Kumai *et al.*, CCL17 and CCL22/CCR4 signaling is a strong candidate for novel targeted therapy against nasal natural killer/T-cell lymphoma. *Cancer Immunol. Immunother.* **64**, 697–705 (2015).
36. Y. Mizukami *et al.*, CCL17 and CCL22 chemokines within tumor microenvironment are related to accumulation of Foxp3+ regulatory T cells in gastric cancer. *Int. J. Cancer* **122**, 2286–2293 (2008).
37. A. Jorapur *et al.*, EBV+ tumors exploit tumor cell-intrinsic and -extrinsic mechanisms to produce regulatory T cell-recruiting chemokines CCL17 and CCL22. *PLoS Pathog.* **18**, e1010200 (2022).
38. T. Nakayama *et al.*, Selective induction of Th2-attracting chemokines CCL17 and CCL22 in human B cells by latent membrane protein 1 of Epstein-Barr virus. *J. Virol.* **78**, 1665–1674 (2004).
39. G. Cortés *et al.*, Identification and quantification of aflatoxins and aflatoxicol from poultry feed and their recovery in poultry litter. *Poultry Sci.* **89**, 993–1001 (2010).
40. G. Tosato, J. I. Cohen, Generation of Epstein-Barr Virus (EBV)-immortalized B cell lines. *Curr. Protoc. Immunol.* **7**, 7 22 1-7 22 4 (2007).
41. C. Wei *et al.*, M2 macrophages confer resistance to 5-fluorouracil in colorectal cancer through the activation of CCL22/PI3K/AKT signaling. *Oncol. Targets Ther.* **12**, 3051–3063 (2019).
42. T. Strowig *et al.*, Priming of protective T cell responses against virus-induced tumors in mice with human immune system components. *J. Exp. Med.* **206**, 1423–1434 (2009).
43. R. E. White *et al.*, EBNA3B-deficient EBV promotes B cell lymphomagenesis in humanized mice and is found in human tumors. *J. Clin. Invest.* **122**, 1487–1502 (2012).
44. Y. Sun *et al.*, Immunotoxicity of three environmental mycotoxins and their risks of increasing pathogen infections. *Toxins (Basel)* **15**, 187 (2023).
45. R. P. Sharma, Immunotoxicity of mycotoxins. *J. Dairy Sci.* **76**, 892–907 (1993).
46. K. He *et al.*, Modulation of inflammatory gene expression by the ribotoxin deoxynivalenol involves coordinate regulation of the transcriptome and translatome. *Toxicol. Sci.* **131**, 153–163 (2012).
47. S. Marchese *et al.*, Aflatoxin B1 and M1: Biological properties and their involvement in cancer development. *Toxins (Basel)* **10**, 241 (2018).
48. Y. Ma *et al.*, Aflatoxin B1 up-regulates insulin receptor substrate 2 and stimulates hepatoma cell migration. *PLoS One* **7**, e47961 (2012).
49. G. Qian *et al.*, Aflatoxin B1 modulates the expression of phenotypic markers and cytokines by splenic lymphocytes of male F344 rats. *J. Appl. Toxicol.* **34**, 241–249 (2014).
50. K. Hieshima *et al.*, Tax-inducible production of CC chemokine ligand 22 by human T cell leukemia virus type 1 (HTLV-1)-infected T cells promotes preferential transmission of HTLV-1 to CCR4-expressing CD4+ T Cells1. *J. Immunol.* **180**, 931–939 (2008).
51. P. Yang *et al.*, TGF-β-miR-34a-CCL22 signaling-induced Treg cell recruitment promotes venous metastases of HBV-positive hepatocellular carcinoma. *Cancer Cell* **22**, 291–303 (2012).
52. T. J. Curiel *et al.*, Specific recruitment of regulatory T cells in ovarian carcinoma fosters immune privilege and predicts reduced survival. *Nat. Med.* **10**, 942–949 (2004).
53. J. Du *et al.*, Spatial transcriptomics analysis reveals that CCL17 and CCL22 are robust indicators of a suppressive immune environment in angioimmunoblastic T cell lymphoma (AITL). *Front. Biosci. (Landmark Ed.)* **27**, 270 (2022).
54. L. Fan *et al.*, SHC014748M, a novel selective inhi-bitor of PI3Kδ, demonstrates promising preclinical antitumor activity in B cell lymphomas and chronic lymphocytic leukemia. *Neoplasia* **22**, 714–724 (2020).
55. K. R. Baumforth *et al.*, Expression of the Epstein-Barr virus-encoded Epstein-Barr virus nuclear antigen 1 in Hodgkin's lymphoma cells mediates Up-regulation of CCL20 and the migration of regulatory T cells. *Am. J. Pathol.* **173**, 195–204 (2008).
56. S. Takegawa *et al.*, Expression of CCL17 and CCL22 by latent membrane protein 1-positive tumor cells in age-related Epstein-Barr virus-associated B-cell lymphoproliferative disorder. *Cancer Sci.* **99**, 296–302 (2008).
57. A. Lavorgna, E. W. Harhaj, EBV LMP1: New and shared pathways to NF-κB activation. *Proc. Natl. Acad. Sci. U.S.A.* **109**, 2188–2199 (2012).
58. L. Hou *et al.*, Immunotoxicity of ochratoxin A and aflatoxin B1 in combination is associated with the nuclear factor kappa B signaling pathway in 3D4/21 cells. *Chemosphere* **199**, 718–727 (2018).
59. S. Kraft, L. Buchenauer, T. Polte, Mold, mycotoxins and a dysregulated immune system: A combination of concern? *Int. J. Mol. Sci.* **22** (2021).
60. N. Diehl, H. Schaal, Make yourself at home: Viral hijacking of the PI3K/Akt signaling pathway. *Viruses* **5**, 3192–212 (2013).
61. J. Tian *et al.*, Blocking the PI3K/AKT pathway enhances mammalian reovirus replication by repressing IFN-stimulated genes. *Front. Microbiol.* **6**, 886 (2015).
62. Q. Rosemarie, B. Sugden, Epstein-Barr virus: How its lytic phase contributes to oncogenesis. *Microorganisms* **8**, 1824 (2020).
63. J. Chen, Roles of the PI3K/Akt pathway in Epstein-Barr virus-induced cancers and therapeutic implications. *World J. Virol.* **1**, 154–161 (2012).
64. M. Granai *et al.*, Burkitt lymphoma with a granulomatous reaction: An M1/Th1-polarised microenvironment is associated with controlled growth and spontaneous regression. *Histopathology* **80**, 430–442 (2022).
65. I. Lecoq *et al.*, CCL22-based peptide vaccines induce anti-cancer immunity by modulating tumor microenvironment. *Oncoimmunology* **11**, 2115655 (2022).
66. D. K. Chang *et al.*, Anti-CCR4 monoclonal antibody enhances antitumor immunity by modulating tumor-infiltrating Tregs in an ovarian cancer xenograft humanized mouse model. *Oncoimmunology* **5**, e1090075 (2016).
67. D. Anz *et al.*, Suppression of intratumoral CCL22 by type i interferon inhibits migration of regulatory T cells and blocks cancer progression. *Cancer Res.* **75**, 4483–4493 (2015).
68. P. Kumar *et al.*, Aflatoxins: A global concern for food safety, human health and their management. *Front. Microbiol.* **7**, 2170 (2016).
69. P. Lopez-Serra, M. Esteller, DNA methylation-associated silencing of tumor-suppressor microRNAs in cancer. *Oncogene* **31**, 1609–1622 (2012).
70. R. C. Vargas-Ayala *et al.*, Interplay between the epigenetic enzyme lysine (K)-specific demethylase 2B and Epstein-Barr virus infection. *J. Virol.* **93**, e00273-19 (2019).

Downloaded from https://www.pnas.org by UNIVERSITEITSBIBLIOTHEEK GENT on June 6, 2024 from IP address 157.193.59.67.